

A HR-like diagram for galaxies: the M_{\bullet} versus $M_G\sigma^2$ relation

A. Feoli

*Dipartimento di Ingegneria, Università del Sannio,
Corso Garibaldi n. 107, Palazzo Bosco Lucarelli
82100 - Benevento, Italy.*

`feoli@unisannio.it`

and

L. Mancini

*Dipartimento di Fisica "E. R. Caianiello", Università di Salerno,
via S. Allende
84081 - Baronissi (SA), Italy.*

`lmancini@physics.unisa.it`

ABSTRACT

We show that the relation between the mass of supermassive black holes located in the center of the host galaxies and the kinetic energy of random motions of the corresponding bulges is a useful tool to study the evolution of galaxies. In the form $\log_{10}(M_{\bullet}) = b + m \log_{10}(M_G\sigma^2/c^2)$, the best-fitting results for a sample of 64 galaxies of various morphological types are the slope $m = 0.80 \pm 0.03$ and the normalization $b = 4.53 \pm 0.13$. We notice that, in analogy with the HR diagram for stars, each morphological type of galaxy generally occupies a different area in the $M_{\bullet} - (M_G\sigma^2)/c^2$ plane. In particular, we find elliptical galaxies in the upper part of the line of best fit, the lenticular galaxies in the middle part, and the late-type galaxies in the lower part, the mass of the central black hole giving an estimate of the age, whereas the kinetic energy of the stellar bulges is directly connected with the temperature of each galactic system. Finally, the values of the linear correlation coefficient and the χ^2 obtained by using the $M_{\bullet} - M_G\sigma^2$ relation are better than the corresponding ones obtained from the $M_{\bullet} - \sigma$ relation.

Subject headings: black hole physics – galaxies: general – galaxies: kinematics and dynamics – galaxies: statistics

1. Introduction

Today the fact that many galaxies, of different morphological types, host a supermassive black hole (SMBH) at their center has been established on quite solid grounds. The studies of the kinematics of galaxies and the combination of multi-band observations have played a major role in this scientific process. At the same time, the idea that the mass of the central SMBH is correlated with the evolutionary state of its host galaxy is being consolidated among the scientific community. In order to qualify this correlation, many relationships have been proposed between the mass of the SMBH and almost all the possible parameters of the host galaxy bulge¹: the velocity dispersion (Ferrarese & Merritt 2000; Gebhardt et al. 2000; Tremaine et al. 2002), the bulge luminosity or mass (Kormendy & Richstone 1995; van der Marel 1999; Richstone et al. 1998; Magorrian et al. 1998; Marconi et al. 2001; Merritt & Ferrarese 2001; Laor 2001; Wandel 2002; Gebhardt et al. 2003; Marconi & Hunt 2003; Häring & Rix 2004; Gültekin et al. 2009b), the galaxy light concentration (Graham et al. 2001), the X-ray power density spectra (Czerny et al. 2001), the dark matter halo (Ferrarese 2002), the radio core length (Cao & Jiang 2002), the effective radius (Marconi & Hunt 2003), the Sersic index (Graham & Driver 2001, 2007), the inner core radius (Lauer et al. 2007), the gravitational binding energy and gravitational potential (Aller & Richstone 2007), the metal abundance (Kisaka et al. 2008), the core mass deficit (Kormendy & Bender 2009), and combination of bulge velocity dispersion, effective radius and/or intensity (Aller & Richstone 2007). An alternative approach has been proposed by Feoli & Mele (2005), who suggested a relation between the black hole mass and the kinetic energy of elliptical galaxies. Then, these authors extended their relation also to lenticular and spiral galaxies (Feoli & Mele 2007), enlarging their sample to a total of 29 galaxies, and finding that it has a scatter smaller than the most famous $M_{\bullet} - \sigma$ relation.

Actually, the main problem is that almost all the above-quoted relations are very tight, so it is very difficult to find, by studying the scatter of each one of them, the “most fundamental one” (Tremaine et al. 2002; Novak et al. 2006; Gültekin et al. 2009b). Without definitely solving this hard problem, the attention of an increasing number of scientists is now focused on the $M_{\bullet} - \sigma$ law in order to study the behavior of some peculiar subsets of galaxies. This led to discover that the line of the best fit of that relationship was different for barred galaxies with respect to the barless ones (Graham 2008). The same occurs for bulges and pseudobulges (Hu 2008), core or coreless (Hu 2008), active or quiescent (Barth et al. 2005; Wyithe 2006a,b; Zhang et al. 2008; Greene & Ho 2006). At the same time, from the theoretical point of view, a lot of interesting models were constructed to explain the experimental results (see for example Haehnelt & Kauffmann (2000); Burkert & Silk (2001); Dokuchaev & Eroshenko (2003)).

A useful method to obtain theoretical predictions, which can be compared with the correlations derived from experimental data, is based on numerical simulations. Hopkins et al. (2007) examined

¹Here *bulge* refers to either the hot, spheroidal component of a spiral/lenticular galaxy or to a full elliptical galaxy

the origin and the evolution of the correlations between properties of SMBHs and their host galaxies using hydrodynamical simulations of major galaxy mergers, including the effects of gas dissipation, cooling, star formation, and black hole accretion and feedback. Their simulations suggest the existence of a SMBH *fundamental plane*, analogous to the fundamental plane of elliptical galaxies. The best relation they find (the one with the lowest scatter) is

$$\log_{10}(M_{\bullet}) = (7.93 \pm 0.06) + (0.72 \pm 0.12) \log_{10}(M_{11}^*) + (1.40 \pm 0.49) \log_{10}(\sigma_{200}), \quad (1)$$

where M_{11}^* is the galaxy stellar mass in units $10^{11} M_{\odot}$, and σ_{200} is the bulge velocity dispersion in units of 200 km/sec. These authors also show the main role played by the kinetic energy of random motions. In particular, they say: “*we therefore naively expect that the BH mass should scale with $M_{*}\sigma^2$* ”, and declare that the correlation between the BH mass and the $M_{*}\sigma^2$ “*is in some sense more basic than the correlation between the BH mass and M_{*} or σ* ”. In other words, their fundamental plane in BH mass can be well represented as a “tilted” correlation between BH mass and the kinetic energy of the random motions in the host galaxies (see Fig. 10 of Hopkins et al. (2007)). Another clue is the ratio between the coefficients in the Eq.(1) multiplying the $\log_{10}(M_{11}^*)$ and $\log_{10}(\sigma_{200})$ which is very close to 0.5. This is also remarked by Marulli et al. (2008), who modelled the cosmological co-evolution of galaxies and their central supermassive black holes within a semi-analytical framework. Their model matches well enough the SMBH fundamental plane relation derived by Hopkins et al. (2007), and their conclusion is identical: the SMBH mass does not simply scale with the star formation (stellar mass) or the velocity dispersion of the host galaxy.

The results of Hopkins et al. (2007) and Marulli et al. (2008) give a strong evidence that galaxy spheroids and SMBHs do not form and evolve independently and support the approach of Feoli & Mele (2005, 2007), who pointed to the relationship between the masses of the SMBHs and the kinetic energy of random motions in their host galaxies. The consequences for the theoretical models of SMBH growth and evolution are non-trivial.

In the present paper we want to extend the previous analysis of Feoli & Mele (2005, 2007) (thereafter Paper I and Paper II) to a new set of 64 galaxies, almost all extracted by the catalogue of Graham (2008). The main aim is to probe if the $M_{\bullet} - M_G \sigma^2$ relation is really a helpful instrument to study the evolution of the galaxies, that is if it can play the same role as the HR diagram in the description of the evolution phases of stars. We will see that different morphological types of galaxies occupy different positions in the $M_{\bullet} - M_G \sigma^2$ plane, reflecting their age and intrinsic features. Finally, we want to confirm that the linear correlation coefficient and the χ^2 of our relationship are better than the corresponding values for the $M_{\bullet} - \sigma$ law. Our paper is structured as follows. In § 2 we define the samples used in our statistics. In § 3 we explain our results with the help of two tables and two figures. Finally, in § 4 we draw our conclusions.

2. The samples

In order to have a homogeneous set of data, we have considered as the main reference for the masses of SMBHs and the velocity dispersions of the galaxies the catalogue published by Graham (2008). This choice involves the values of the central velocity dispersions, in contrast with our two previous papers where we used the effective dispersion velocity. As already noted by Novak et al. (2006), the two ways of measuring the velocity dispersion does not generate profound differences. This is also supported by the study of Hu (2008), who compared the effective dispersion σ_e with the central one σ_c , finding that the differences are much smaller than their measurement errors. We also remark the fact that in our previous papers the data were extracted only by single sources: in Paper I all the values of the galaxies masses have been taken from Curir et al. (1993), the velocity dispersions from Busarello et al. (1992), and the SMBH masses from Tremaine et al. (2002); in Paper II the three sets of data have been taken from Häring & Rix (2004). Here, due to the enlargement of the sample, a homogeneous choice is no more possible and we are forced to build up a sample of data from various catalogues – essentially those of Graham (2008), Häring & Rix (2004) and Cappellari et al. (2006) – and single papers. A clear limit of a collection of data of this kind is, of course, related to the many different techniques utilized to estimate the masses of the bulge (dynamical or virial masses, Schwarzschild models, Jeans equation, etc.) and of the SMBHs (gas or stellar kinematics, water maser, proper motions, etc.).

In this paper, we consider two samples of galaxies. The first sample (sample A) is composed by 49 galaxies included in the table 1 of Graham (2008). Actually, his catalogue is formed by 50 galaxies that are considered to have reasonable measurements of their SMBH masses. We exclude the galaxy IC2560, since a reliable value for its bulge mass is not available (Ishihara et al. 2001; Schulz & Henkel 2003). In several cases we would have liked to substitute some data of the Graham catalogue with other measures which, in our opinion, are less uncertain or simply more recent, but we did not do so in order to avoid the risk that the tightness of our relation might depend on a suitable choice of the data. For example, we have used for the mass of SMBH in Milky Way the value cited by Graham even if we know that an update value is now available (Gillessen et al. 2009) and we have included in the sample also the elliptical NGC221, which we would have liked to exclude from the fit as already done in Paper I and II. Starting from the Graham’s catalogue we have fixed the total number and the names of galaxies, their velocity dispersions, the SMBH masses, and morphological types. In this way, only the galaxy mass remains as a free parameter but our choice was anyway restricted by using the data published by Häring & Rix (2004) and Cappellari et al. (2006).

The second sample (sample B) is composed by the galaxies of the sample A plus other 15 galaxies whose parameters have been taken from table 2 of Graham (2008) and from other papers. Of course, this enlarged sample does have not the aim to include all the galaxies with a measured BH mass or with an upper limit on its value. 64 galaxies are listed in Table 1 and compose the sample B, while only the first 49 galaxies are included in the sample A.

Concerning the errors in the measures, we adopt the same strategy as in Paper II. Following Häring & Rix (2004), we consider that the error for the bulge mass is 0.18 dex in $\log_{10} M_G$ for all the galaxies, while the relative error on the velocity dispersions is 10%, as in Graham (2008).

3. Results

The relation between the mass of the SMBHs and the kinetic energy of random motions of the corresponding host galaxies has been presented in Paper I and II in the form

$$\log_{10}(M_\bullet) = b + m \log_{10}(M_G \sigma^2 / c^2). \quad (2)$$

Thus, this relation can be used to predict the values of M_\bullet in other galaxies once we know their mass and velocity dispersion. In order to minimize the scatter in the quantity to be predicted, we have to perform an ordinary least-squares regression of M_\bullet on $M_G \sigma^2$ for the galaxies in Table 1, of which we already know both the quantities. In Table 2 we compare the fits of our relationship for the two samples and the corresponding fits for $M_\bullet - \sigma$ law. As in Paper II (see also Graham & Driver (2007)), these fits were obtained taking into account the error bars in both variables and using the routine FITEXY (Press et al. 1992) for a relation $y = b + mx$, by minimizing the χ^2 (see Appendix A). The best-fitting lines of the $M_\bullet - M_G \sigma^2$ relation for the the samples A and B are shown in Figures 1 and 2 respectively. Comparing the results of the two laws, we notice that the χ^2 and the Pearson linear correlation coefficient r of our relationship are better than the other one. Furthermore, comparing the results in Table 2 with the corresponding ones in table 3 of Paper II, we observe that, by enlarging the sample, the correlation coefficient of our relationship increases, showing the robustness of our idea.

As already observed by Novak et al. (2006) the question “which relation is better than the others?” is extremely sensitive to inaccurate estimates of measurement errors. So, the result that our χ^2 is better than the $M_\bullet - \sigma$ law can be caused by an overestimation of the error on the galaxy masses. In order to avoid a similar misleading result, we have checked what happens using a standard least squared fitting, assuming that errors in the kinetic energy are zero and that errors in the $\log_{10} M_\bullet$ are the same ϵ_y for each galaxy. The results are reported in Table 3 and show that the scatter of our relationship is better than the $M_\bullet - \sigma$ law even in this extremal case. Furthermore the slope of the line of best fit $m = 0.73 \pm 0.04$ is the same, inside the errors, as the one of (Hopkins et al. 2007) in the Eq. (1).

A surprising result is shown in Figure 1 where the galaxies of sample A are reported. We perform a log - log plot of the energy stored by the SMBH, $E_{st} = M_\bullet c^2$, as a function of the bulge kinetic energy of random motions, both normalized by the rest energy of the Sun, $M_\odot c^2$. To each galaxy we associated a particular marker according with its morphological type. Given the line of best fit (solid line) and a sort of border line (dashed line) that divides the diagram in two parts, it is evident that:

1. Almost all the elliptical galaxies (except NGC3377) are in the higher part of the diagram (over the dashed line).
2. The lenticular galaxies are located in the middle-upper part of the diagram.
3. The barred lenticular galaxies are located in the middle part of the diagram (but under the dashed line).
4. All the spirals are in the middle-lower and in the lower parts of the diagram (under the dashed line).
5. In the lower part of the diagram we find also two dwarf elliptical galaxies: NGC221 and NGC4486A.

An identical diagram is reported in Figure 2 for the galaxies of the sample B. The general trend observed in Figure 1 is respected, even if two lenticular galaxies appear in the lower part of the diagram and a spiral galaxy in the upper part. The latter is the famous *Sombbrero galaxy* (NGC4594), one of the largest galaxies in the nearby Virgo Cluster, classified as a lenticular by Magorrian et al. (1998). It is well known that it has a bright nucleus and an unusually large classical bulge, testified by a relatively large number of globular clusters. We know that the classical bulges are believed to be generated by mergers and are common in early type galaxies but become progressively rare towards later types. They share some structural, dynamical and population properties with the lower-luminosity ellipticals (Freeman 2007). Actually, NGC4594 is surrounded by a halo of stars, dust and gas that indicate it may actually be described as an elliptical galaxy that contains a more robust interior configuration. Therefore, its presence in the upper part of the diagram is not so improper. Later type galaxies like the Milky Way mostly have small boxy bulges and are all in the lower part of the diagram. On the other side, both a classical bulge and an inner boxy bulge are present in NGC224 (Andromeda galaxy, M31) (Athanasoulas & Beaton 2006; Beaton et al. 2007), which is located just the middle region.

In both the figures, the elliptical galaxies are all clustered very near the line of best fit. Conversely, the galaxies of the other morphological types look slightly more scattered. This is particularly true for the lenticular galaxies in the middle-upper part of the diagram. Among them, the galaxy NGC4342 is located quite far from the best-fitting line. As already noted by Cretton & van den Bosch (1999), NGC4342 is one of the galaxies with the highest SMBH mass to bulge mass ratio. The consequent hypothesis that we are in presence of a galaxy in a particular evolutionary state is also supported by the presence of both an outer disk and a stellar nuclear disk (van den Bosch & Jaffe 1997). Instead, the position of the lenticular galaxy NGC7457 in the lower zone of the diagram is due to its SMBH which is one of the least-massive black holes yet detected in the core of a galaxy, roughly the same mass as the black hole at the center of our Galaxy. Equally, the boxy-bulge lenticular NGC7332 is located in the middle-lower region of the Figure 2. Going on, the peculiar galaxy NGC5128 (Centaurus A) appears in the middle of the diagram, but still quite far from the other lenticulars. The strange morphology of Centaurus A is

generally recognized as the result of a merger of two smaller galaxies. In this way, it is possible to explain a bulge comprised mainly of evolved red stars and a dusty disk, which has been the site of recent star formation (Israel 1998).

Finally, we note the presence of the intermediate-size elliptical NGC3377 in the center of the graphic in Figure 2, and three dwarf elliptical galaxies in the lower part. Two of them are NGC4742 and NGC4486A, both belonging to the Virgo Cluster of Galaxies, whereas the small NGC221 (M32) is a satellite of M31. Continuing the analogies with the HR diagram, we can look at this area as reserved to the dwarf ellipticals, in the same manner as the region occupied by the white dwarfs in a classical color-magnitude diagram. If the three dwarf ellipticals do not really belong to the “principal sequence” we can exclude them from the fit. In this case the slope and the normalization in our relationship for the reduced sample of 61 galaxies are 0.84 ± 0.03 and 4.33 ± 0.15 respectively (dashed line in Figure 2). Further more, comparing again the $\chi_r^2 = 1.80$ and the $r = 0.91$ of our relation with the corresponding $\chi_r^2 = 2.37$ and $r = 0.83$ for the $M_\bullet - \sigma$ law, we find an increase of the gap between the two relations.

Also remarkable is the fact that all the barred galaxies (lenticulars and spirals) are located only in the lower/middle-lower part of the diagram (under the dashed line of Figure 1).

We also study a possible correlation between the activity (Seyfert, Liner, etc.) of each galaxy with its position on the diagram, but we did not note any particular trend.

4. Discussion

In this paper we have investigated the relation between the mass of the SMBHs and the kinetic energy of the random motion of the corresponding galaxies. This relation has been tested on a homogeneous sample of 49 galaxies and then on a more enlarged sample of 64 ones. As shown in Table 1, the statistical analysis confirms the result of our two previous papers, that is the proposed relation works well and better than the most common $M_\bullet - \sigma$ law. Furthermore, the main result that we report consists in the particular positions of the galaxies in the $M_\bullet - (M_G \sigma^2)/c^2$ plan, which resembles the HR diagram for the stars. The analogies between the two diagrams are the following.

The HR diagram connects the energy radiated (per unit time) by the nucleus of a star with its surface temperature. In the same way, our diagram connects a property of the inner nucleus of a galaxy, the energy stored by the SMBH, $M_\bullet c^2$, with a property of the external surface of its bulge, i.e. the kinetic energy of random motions. This energy is related just with the temperature of the stellar system. In fact, let us consider a spherically symmetric distribution of stars with density ρ , whose dynamical state is described by a distribution function of the form

$$F(E) = \frac{\rho}{(2\pi\sigma^2)^{3/2}} e^{E/\sigma^2}, \quad (3)$$

where $E = \Psi - v^2/2$ is the binding energy, and Ψ is the relative gravitational potential (Binney & Tremaine 1987). Now, it is well known that the structure of a collisionless system of stars, whose density in the phase space is given by Eq. (3), is identical to the structure of an isothermal self-gravitating sphere of gas, if we set

$$M\sigma^2 = Nk_{\text{B}}T, \quad (4)$$

M being the total mass of the system, N the number of objects contained in the system, and k_{B} the Boltzmann's constant. Since a stellar bulge can be considered, with a good approximation, similar to a spherically symmetric system, its kinetic energy of the random motions $M_G\sigma^2$ gives an indication of the temperature of the galaxy bulge. On the other side, since the SMBH at the center of galaxies can only increase its mass, the stored energy is directly connected with the initial density of the system and its evolutionary state. So, the stored energy of central SMBH will guide the galaxy along the evolutionary process, and, in that sense, an accretion of the SMBH, bound up with the flow of time, will imply a migration of the galaxy position from the lower-right part of the $M_{\bullet} - (M_G\sigma^2)$ diagram to the upper-left.

We are grateful to Federico Marulli and Gianni Busarello for useful discussions and to Michele Cappellari for a private communication about the values of some galaxy masses. This research was partially supported by FAR fund of the University of Sannio. L.M. acknowledges support for this work by MIUR through PRIN 2006 Protocol 2006023491_003, by research funds of Agenzia Spaziale Italiana, by funds of Regione Campania, L.R. n.5/2002, year 2005 (run by Gaetano Scarpetta), and by research funds of Salerno University.

A. Appendix

The formula used in this paper to estimate the maximal errors in the functions F of the parameters (a, b, c, \dots) is

$$\Delta F(a, b, c) = \left| \frac{\partial F}{\partial a} \right| \Delta a + \left| \frac{\partial F}{\partial b} \right| \Delta b + \left| \frac{\partial F}{\partial c} \right| \Delta c. \quad (\text{A1})$$

The reduced χ^2 , used in table 2, is defined as

$$\chi_r^2 = \frac{\chi^2}{N-2} = \frac{1}{N-2} \sum_{i=1}^N \frac{(y_i - b - mx_i)^2}{(\Delta y_i)^2 + m^2(\Delta x_i)^2}, \quad (\text{A2})$$

for a relation of the form $y = b + mx$, where N is the number of galaxies in the sample.

Furthermore ϵ_y , used in Table 3, is defined as

$$\epsilon_y^2 = \frac{1}{N-2} \sum_{i=1}^N (y_i - b - mx_i)^2. \quad (\text{A3})$$

Finally, the Pearson linear correlation coefficient is

$$r = \frac{\sum_{i=1}^n (x_i - \bar{x})(y_i - \bar{y})}{\sqrt{\sum_{i=1}^n (x_i - \bar{x})^2} \sqrt{\sum_{i=1}^n (y_i - \bar{y})^2}} . \quad (\text{A4})$$

REFERENCES

- Aller, M. C., Richstone, D. O. 2007, *ApJ*, 665, 120
- Athanassoula, E., & Beaton, R. L. 2006, *MNRAS*, 370, 1499
- Atkinson, J.H., Kazeminejad, B., Gaborit, V., et al. *MNRAS*, 359, 504
- Bacon, R., Monnet, G., Simien, F. 1985, *A&A*, 152, 315
- Barth, A. J., Greene, J. E., Ho, L. C. 2005, *ApJ*, 619, L151
- Batcheldor, D., Axon, D., Merritt, D., et al. 2005, *ApJS*, 160, 76
- Beaton, R., Majewski, S., Patterson, R., et al. 2007, *ApJ*, 658, L91
- Bekki, K., Harris, W. E., & Harris, G. L. H., et al. 2003, *MNRAS*, 338, 587
- Binney, J., & Tremaine, S. 1987, *Galactic Dynamics* (Princeton NJ, Princeton Univ. Press)
- Burkert, A. & Silk, J. 2001, *ApJ*, 554, L151
- Busarello, G., Longo, G. & Feoli, A. 1992, *A&A*, 262, 52
- Cappellari, M., Bacon, R., Bureau, M., et al. 2006, *MNRAS*, 366, 1126
- Cappellari, M. 2009, private communication
- Cao, X. & Jiang, D. R. 2002, *MNRAS*, 331, 111
- Cretton, N., van den Bosch, F. C. 1999, ASP Conference Series vol. 182, edited by Merritt, D. R., Valluri, M., & Sellwood, J. A. (San Francisco: ASP), p.41
- Curir, A., De Felice, F., Busarello, G., & Longo, G. 1993, *Astrophys. Lett. Commun.*, 28, 323
- Czerny, B., Nikolajuk, M., Piasecki, M., & Kuraszkievicz, J. 2001, *MNRAS*, 325, 865
- Dalla Bontà, E., Ferrarese, L., Corsini, E. M., et al. 2007, *Mem. S.A.It.*, 78, 745
- De Francesco, G., Capetti, A., & Marconi, A. 2006, *A&A*, 460, 439
- De Francesco, G., Capetti, A., & Marconi, A. 2008, *A&A*, 479, 355
- Dokuchaev, V. I. & Eroshenko, Yu. N. 2003, *A&AT*, 22, 727
- Feoli, A. & Mele, D. 2005, *Int. Jour. Mod. Phys. D*, 14, 1861
- Feoli, A. & Mele, D. 2007, *Int. Jour. Mod. Phys. D*, 16, 1261
- Ferrarese, L., & Merritt, D. 2000, *ApJ*, 539, L9

- Ferrarese, L. 2002, *ApJ*, 578, 90
- Freeman, K. C. 2007, *Proceedings of IAU Symposium #245*, edited by Bureau, M., Athanassoula, E., & Barbuy, B., Univ. Press, Cambridge, p.3
- Gebhardt, K., Bender, R., Bower, G., et al. 2000, *ApJ*, 539, 13
- Gebhardt, K., Richstone, D., Tremaine, S., et al. 2003, *ApJ*, 583, 92
- Gillessen, S., Eisenhauer, F., Trippe, S., et al. 2009, *ApJ*, 692, 1075
- Genzel, R., Weitzel, L., Tacconi-Garman, L. E., et al. 1995, *ApJ*, 444, 129
- Graham, A.W., Erwin, P., Caon, N., & Trujillo, I. 2001, *ApJ*, 563, L11
- Graham, A.W., & Driver, S. P. 2005, *PASA*, 22(2), 118
- Graham, A. W., & Driver, S. P. 2007, *ApJ*, 655, 77
- Graham, A. W. 2008, *PASA*, 25, 167
- Greene, J. E. & Ho, L. C. 2006, *ApJ*, 641, L21
- Gultekin, K., Richstone, D. O., Gebhardt, K., et al. 2009a, to appear on *ApJ*, arXiv0901.4162
- Gultekin, K., Richstone, D. O., Gebhardt, K., et al. 2009b, to appear on *ApJ*, arXiv0903.4897
- Haehnelt, M. G. & Kauffmann, G. 2000, *MNRAS*, 318, L35
- Häring, N., & Rix, H. 2004, *ApJ*, 604, L89
- Hicks, E. K. S., & Malkan, M. A. 2008, *ApJS*, 174, 31
- Hitschfeld, M., Aravena, M., Kramer, C., et al. 2008, *A&A*, 479, 75
- Houghton, R. C. W., Magorrian, J., Sarzi, M., et al. 2006, *MNRAS*, 367, 2
- Hopkins, P. F., Hernquist, L., Cox, T. J., et al. 2007, 669, 45
- Hu, J. 2008, *MNRAS*, 386, 2242
- Ishihara, Y., Nakai, N., Iyomoto, N., et al. 2001, *PASJ*, 53, 215
- Israel, F. P. 2009, *A&A*, 493, 525
- Israel, F. P. 1998, *A&ARv*, 8, 237
- Kisaka, S., Kojima, Y., & Otani, Y. 2008, *MNRAS*, 390, 814
- Koda, J., Sofue, Y., Kohno, K., et al. 2002, *ApJ*, 573, 105

- Kormendy, J., & Richstone, D. 1995, *ARA&A*, 33, 581
- Kormendy, J., & Bender, R. 2009, *ApJ*, 691, L142
- Laor, A., 2001, *ApJ*, 553, 677
- Lauer, T. R., Faber, S. M., Richstone, D. 2007, *ApJ*, 662, 808
- Magorrian, J., Tremaine, S., Richstone, D., et al. 1998, *AJ*, 115, 2285
- Marconi, A., Axon, D., Atkinson, J., et al. 2001, *Proceedings of IAU Symposium #205*, edited by Schilizzi, R. T., Vogel, S. N., Paresce, F., & Elvis, M. S. (San Francisco: ASP), p.58
- Marconi, A., & Hunt, L. K. 2003, *ApJ*, 589, L21
- Marulli, F., Bonoli, S., Branchini, E. 2008, *MNRAS*, 385, 1846
- Merritt, D., & Ferrarese, L. 2001, *ASP Conference Proceedings Vol. 249*, edited by Knapen, J. H., Beckman, J. E., Shlosman, I., & Mahoney, T. J. (San Francisco: ASP, 2001), p.335
- Novak, G. S., Faber, S. M. & Dekel, A. 2006, *ApJ*, 637, 96
- Nowak, N., Saglia, R. P., Thomas, J., et al., *MNRAS*, 379, 909 (2007)
- Peterson, B. M., Ferrarese, L., Gilbert, K. M., et al. 2004, *ApJ*, 613, 682
- Press, W. H., Teukolsky, S. A., Vetterling, W. T. & Flannery, B. P. 1992, *Numerical Recipes* (2nd ed.; Cambridge: Cambridge Univ. Press)
- Richstone, D., Ajhar, E. A., Bender, R., et al. 1998, *Nature*, 395, A14
- Riffeser, A., Seitz, S., & Bender, R. 2008, *ApJ*, 684, 1093
- Sarzi, M., Rix, H.-W., Shields, J. C., et al. 2001, *ApJ*, 550, 65
- Schulz, H., & Henkel, C. 2003, *A&A*, 400, 41
- Sofue, Y. 1998, *PASJ*, 50, 227
- Tremaine, S., Gebhardt, K., Bender, R., et al. 2002, *ApJ*, 574, 740
- van den Bosch, F. C., & Jaffe, W. 1997, *ASP Conference Series, Vol. 116*, edited by Arnaboldi, M., Da Costa, G. S., & Saha, P., p.142
- van der Marel, R. P. 1999, *Proceedings of IAU Symp. 186*, edited by Sanders, D. B., & Barnes, J. (Dordrecht: Kluwer Academic Publishers), p.333
- Wandel, A. 1999, *ApJ*, 519, L39
- Wandel, A. 2002, *ApJ*, 565, 762

- Wold, M., Lacy, M., Käufel, H. U., et al. 2006, *A&A*, 460, 449
- Wyithe, J. S. B. 2006a, *MNRAS*, 365, 1082
- Wyithe, J. S. B. 2006b, *MNRAS*, 371, 1536
- Zhang, S.-Y., Bian, W.-H., Huang, K.-L. 2008, *A&A*, 488, 113

Table 1. Sample

Galaxy	Type ^a	σ_c (km/s)	References	M_\bullet (M_\odot)	δM_\bullet (M_\odot)	References	M_G (M_\odot)	References
CygnusA	E	270	1	2.5×10^9	7.0×10^8	1	1.6×10^{12}	2
NGC221	E2	72	1	2.5×10^6	5.0×10^5	1	8.0×10^8	4
NGC821	E6	200	1	8.5×10^7	3.5×10^7	1	1.3×10^{11}	4
NGC1399	E1	329	1	4.8×10^8	7.0×10^7	1	2.32×10^{11}	22
NGC2974	E4	227	1	1.7×10^8	3.0×10^7	1	1.57×10^{11}	10
NGC3377	E5	139	1	8.0×10^7	6.0×10^6	1	3.08×10^{10}	10
NGC3379	E1	207	1	1.4×10^8	2.7×10^8	1	6.8×10^{10}	4
NGC3608	E2	192	1	1.9×10^8	1.0×10^8	1	9.7×10^{10}	4
NGC4261	E2	309	1	5.2×10^8	1.1×10^8	1	3.6×10^{11}	4
NGC4291	E2	285	1	3.1×10^8	2.3×10^8	1	1.3×10^{11}	4
NGC4374	E1	281	1	4.64×10^8	3.46×10^8	1	3.6×10^{11}	4
NGC4473	E5	179	1	1.1×10^8	8.0×10^7	1	9.2×10^{10}	4
NGC4486	E0	332	1	3.4×10^9	1.0×10^9	1	6.0×10^{11}	4
NGC4486A	E2	110	1	1.3×10^7	8.0×10^6	1	4.06×10^9	11
NGC4621	E5	225	1	4.0×10^8	6.0×10^7	1	1.88×10^{11}	10
NGC4649	E1	335	1	2.0×10^9	6.0×10^8	1	4.9×10^{11}	4
NGC4697	E4	174	1	1.7×10^8	2.0×10^7	1	1.1×10^{11}	4
NGC5077	E3	255	1	7.4×10^8	4.7×10^8	1	2.1×10^{11}	12
NGC5813	E1	239	1	7.0×10^8	1.1×10^8	1	5.05×10^{11}	10
NGC5845	E3	233	1	2.4×10^8	1.4×10^8	1	3.7×10^{10}	4
NGC5846	E0	237	1	1.1×10^9	2.0×10^8	1	6.36×10^{11}	10
NGC6251	E2	311	1	5.9×10^8	2.0×10^8	1	5.6×10^{11}	4
NGC7052	E4	277	1	3.7×10^8	2.6×10^8	1	2.9×10^{11}	4
NGC3115	S0	252	1	9.1×10^8	1.03×10^9	1	1.2×10^{11}	4
NGC3245	S0	210	1	2.1×10^8	5.0×10^7	1	6.8×10^{10}	4
NGC3414	S0	237	1	2.5×10^8	4.0×10^7	1	1.7×10^{11}	10
NGC3998	S0	305	1	2.2×10^8	2.0×10^8	1	5.5×10^{10}	13
NGC4342	S0	253	1	3.3×10^8	1.9×10^8	1	1.2×10^{10}	4
NGC4459	S0	178	1	7.0×10^7	1.3×10^7	1	7.86×10^{10}	10
NGC4552	S0	252	1	4.8×10^8	8.0×10^7	1	1.87×10^{11}	10
NGC4564	S0	157	1	5.6×10^7	3.0×10^6	1	4.4×10^{10}	4
NGC5128	S0	120	1	4.9×10^7	1.8×10^7	1	2.16×10^{10}	23
NGC5252	S0	190	1	1.06×10^9	1.63×10^9	1	2.4×10^{11}	2
NGC1023	SB0	204	1	4.4×10^7	5.0×10^6	1	6.9×10^{10}	4
NGC2778	SB0	162	1	1.4×10^7	9.0×10^6	1	1.06×10^{10}	25
NGC2787	SB0	210	1	4.1×10^7	5.0×10^6	1	2.9×10^{10}	5
NGC3384	SB0	148	1	1.6×10^7	2.0×10^6	1	2.0×10^{10}	4
NGC4596	SB0	149	1	7.9×10^7	3.8×10^7	1	2.6×10^{10}	2
Circinus	S	75	1	1.1×10^6	2.0×10^5	1	3.0×10^9	15
NGC224	SA	170	1	1.4×10^8	9.0×10^7	1	4.4×10^{10}	16
NGC3031	SA	162	1	7.6×10^7	2.2×10^7	1	1.0×10^{10}	17
MW	SB	100	1	3.7×10^6	2.0×10^5	1	1.1×10^{10}	4
NGC1300	SB	229	1	7.3×10^7	6.9×10^7	1	2.14×10^{10}	7
NGC3079	SB	146	1	2.4×10^6	2.4×10^6	1	1.7×10^9	18
NGC3227	SAB	133	1	1.4×10^7	1.0×10^7	1	2.95×10^9	19

Table 1—Continued

Galaxy	Type ^a	σ_c (km/s)	References	M_\bullet (M_\odot)	δM_\bullet (M_\odot)	References	M_G (M_\odot)	References
NGC4151	SAB	156	1	6.5×10^7	7.0×10^6	1	1.09×10^{11}	26
NGC4258	SAB	134	1	3.9×10^7	1.0×10^6	1	1.1×10^{10}	2
NGC4945	SB	100	1	1.4×10^6	1.4×10^6	1	3.0×10^9	15
NGC7582	SB	156	1	5.5×10^7	2.6×10^7	1	1.31×10^{11}	9
IC1459	E3	306	1	1.5×10^9	1.0×10^9	2	6.6×10^{11}	2
IC4296	E	336	1	1.3×10^9	4.0×10^8	1	1.56×10^{12}	20
NGC3607 ^b	E	229	3	1.2×10^8	4.0×10^7	3	2.70×10^{11}	3
NGC4486B	E0	169	1	6.0×10^8	3.0×10^8	1	1.22×10^{11}	24
NGC4742	E4	109	1	1.4×10^7	5.0×10^6	1	6.2×10^9	4
NGC5576 ^b	E3	183	3	1.8×10^8	4.0×10^7	3	1.47×10^{11}	3
NGC3585 ^b	S0	213	3	3.4×10^8	1.5×10^8	3	1.85×10^{11}	3
NGC4026 ^b	S0	180	3	2.1×10^8	7.0×10^7	3	5.17×10^{10}	3
NGC7332	S0	135	1	1.3×10^7	6.0×10^6	1	1.5×10^{10}	4
NGC7457	S0	69	1	3.5×10^6	1.4×10^6	1	7.0×10^9	4
NGC4203	SB0	124	5	5.2×10^7	1.0×10^6	5	1.5×10^{10}	5
NGC1068	SA	151	1	8.4×10^6	3.0×10^5	1	1.5×10^{10}	21
NGC2748	SA	79	6	4.4×10^7	3.6×10^7	7	1.69×10^{10}	7
NGC4594	SA	240	1	1.0×10^9	1.0×10^9	4	2.7×10^{11}	4
NGC7469	SAB	152	8	1.22×10^7	1.40×10^6	8	4.5×10^9	14

References. — (1) Graham (2008); (2) Marconi & Hunt (2003); (3) Gultekin et al. (2009a); (4) Häring & Rix (2004); (5) Sarzi et al. (2001); (6) Batcheldor et al. (2005); (7) Atkinson et al. (2005); (8) Hicks & Malkan (2008); (9) Wold et al. (2006); (10) Cappellari et al. (2006), Cappellari (2009); (11) Nowak et al. (2007); (12) De Francesco et al. (2008); (13) De Francesco et al. (2006); (14) Genzel et al. (1995); (15) Hitschfeld et al. (2008); (16) Riffeser et al. (2008); (17) Sofue (1998); (18) Koda et al. (2002); (19) Wandel (2002); (20) Dalla Bontà et al. (2007); (21) Israel (2009); (22) Houghton et al. (2006); (23) Bekki et al. (2003); (24) Bacon et al. (1985); (25) Aller & Richstone (2007); (26) Wandel (1999).

Note. — ^bGalaxy types are taken from Graham (2008) with the following exceptions: IC4296, NGC221, NGC821, NGC1399, NGC2974, NGC3379, NGC3607, NGC4374, NGC4486A, NGC4486B, NGC4621, NGC5077, NGC5813, NGC5846, NGC6251, which are taken from the NASA/IPAC Extragalactic database. ^bEffective dispersion σ_e is given rather than the central σ_c .

Table 2.

Relation (1)	Sample (2)	N (3)	$m \pm \Delta m$ (4)	$b \pm \Delta b$ (5)	χ_r^2 (6)	r (7)
$M_\bullet - M_G \sigma^2$	A	49	0.80 ± 0.03	4.49 ± 0.15	1.74	0.92
$M_\bullet - \sigma$	A	49	5.06 ± 0.25	8.18 ± 0.04	1.85	0.87
$M_\bullet - M_G \sigma^2$	A	64	0.80 ± 0.03	4.53 ± 0.13	1.92	0.92
$M_\bullet - \sigma$	A	64	5.00 ± 0.21	8.20 ± 0.04	2.34	0.85

Note. — We report the used relation in column (1), the sample in column (2), and the corresponding number of galaxies in column (3). By using the routine FITEXY, we find the best fit of the relationship $y = b + mx$. The results for m and b are in column (4) and (5) and the corresponding reduced $\chi_r^2 = \chi^2/(N - 2)$ in column (6). Finally, the linear correlation coefficient is shown in column (7).

Table 3.

Relation (1)	Sample (2)	N (3)	$m \pm \Delta m$ (4)	$b \pm \Delta b$ (5)	ϵ_y^2 (6)
$M_\bullet - M_G \sigma^2$	A	49	0.74 ± 0.04	4.80 ± 0.20	0.10
$M_\bullet - \sigma$	A	49	4.46 ± 0.36	8.13 ± 0.06	0.16
$M_\bullet - M_G \sigma^2$	B	64	0.73 ± 0.04	4.88 ± 0.18	0.11
$M_\bullet - \sigma$	B	64	4.12 ± 0.32	8.17 ± 0.06	0.19

Note. — We report the used relation in column (1), the sample in column (2), and the corresponding number of galaxies in column (3). By using a standard least squared fitting and assuming that errors in the galaxy mass and velocity dispersion are zero and that errors in the $\log_{10} M_\bullet$ are the same ϵ_y for each galaxy, we find the best fit of the relationship $y = b + mx$. The results for m and b are in column (4) and (5) respectively. The values of the ϵ_y are in column (6).

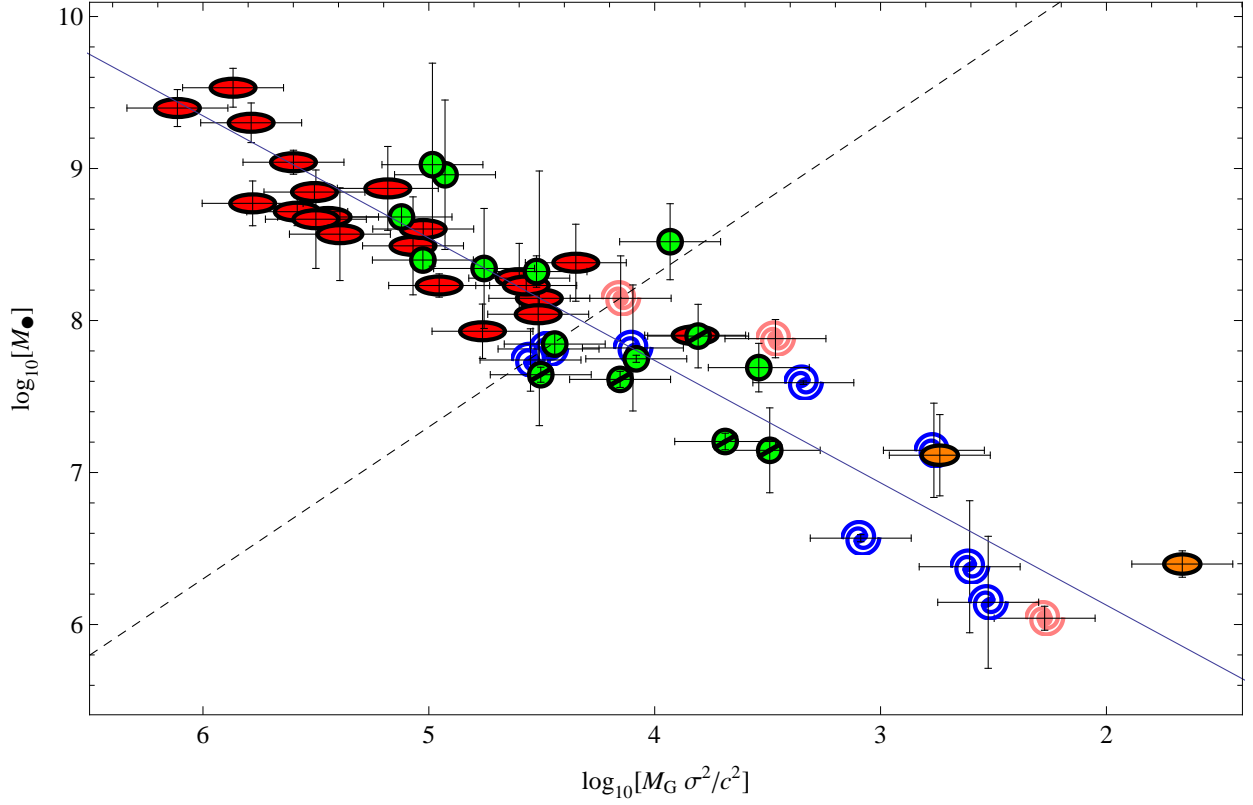


Fig. 1.— The best-fitting $M_{\bullet} - M_G \sigma^2$ relation for the elliptical galaxies (red ellipses), lenticular galaxies (green circles), barred lenticular galaxies (green barred circles), spiral galaxy (pink spirals), barred spiral galaxies (blue barred spirals), and dwarf elliptical galaxies (orange round ellipses) of the sample A.

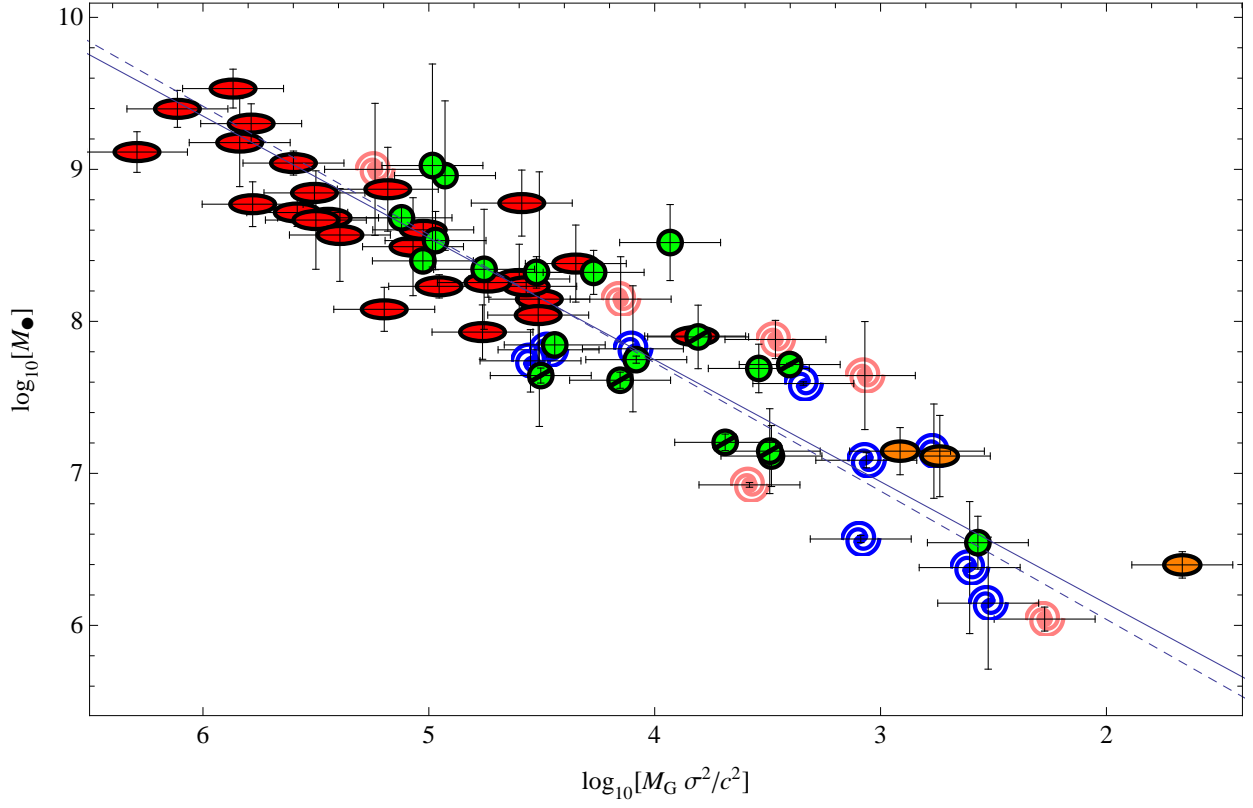


Fig. 2.— For the $M_{\bullet} - M_G \sigma^2$ relation, the line of best fit for the galaxies of sample B is represented by a solid line, whereas the one obtained without considering the three dwarf ellipticals by a dashed line. The markers are the same of Figure 1.